Electronic Supplementary Material (ESI) for Chemical Communications

Cerium oxide nanoparticle-mediated self-assembly of hybrid supramolecular hydrogels†

Avinash J. Patil*, Ravinash Krishna Kumar, Nicholas J. Barron and Stephen Mann*

Supplementary Information

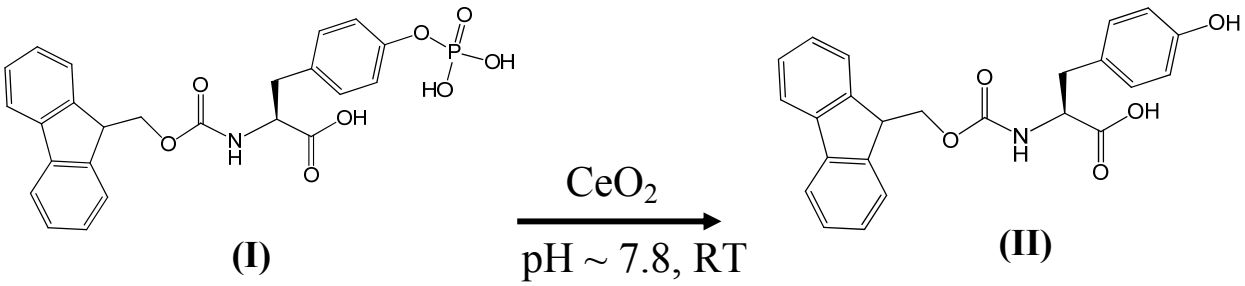

Scheme 1. Chemical structures of amino acid reactant, FMOC-Tyr-P (**I**) and cerium oxide nanoparticle catalyzed dephosphorylated product, FMOC-Tyr (**II**).

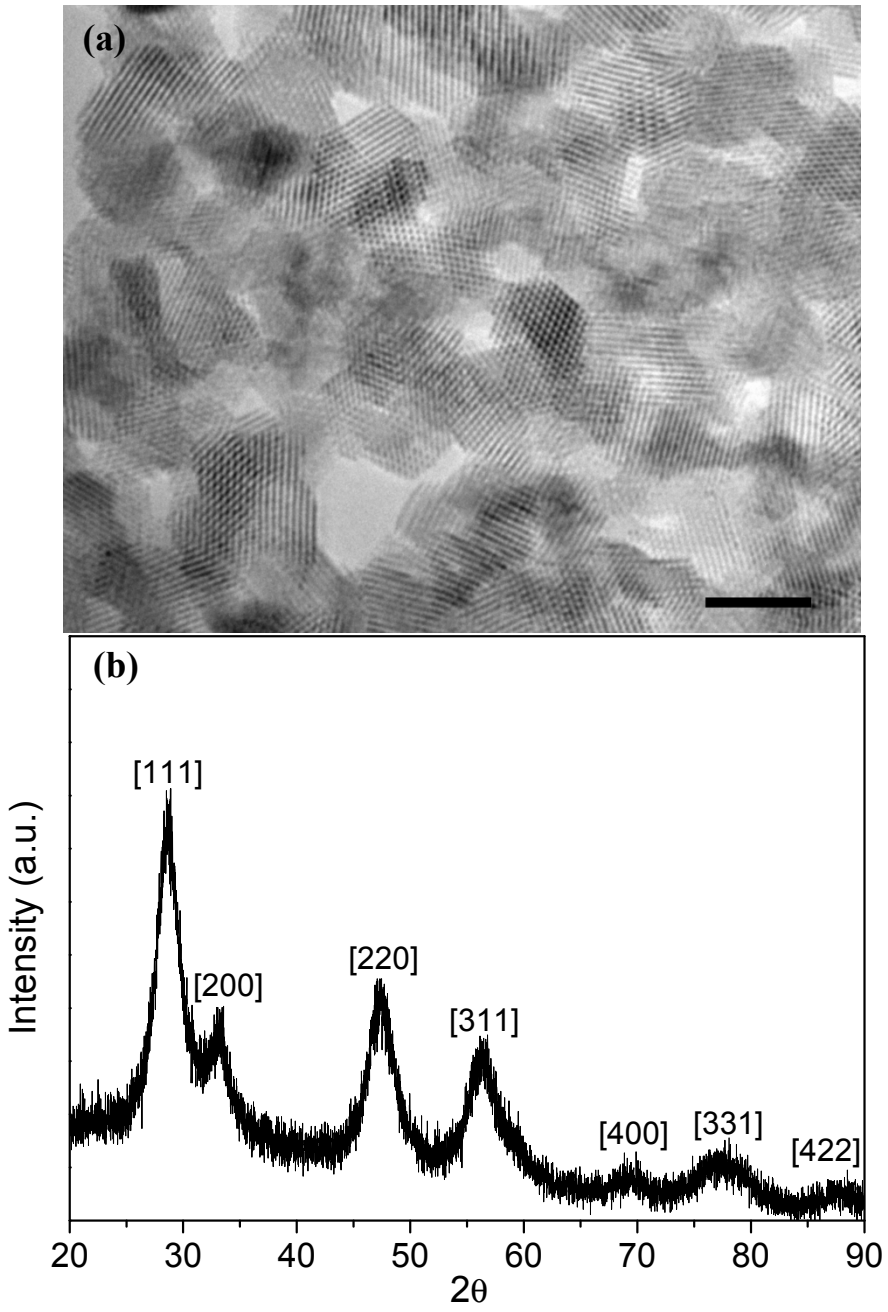

Figure S1: (a) High resolution TEM image of cerium oxide nanoparticles showing well defined {111} lattice fringes corresponding to the cubic fluorite structure, scale bar = 5 nm. (b) corresponding PXRD pattern.

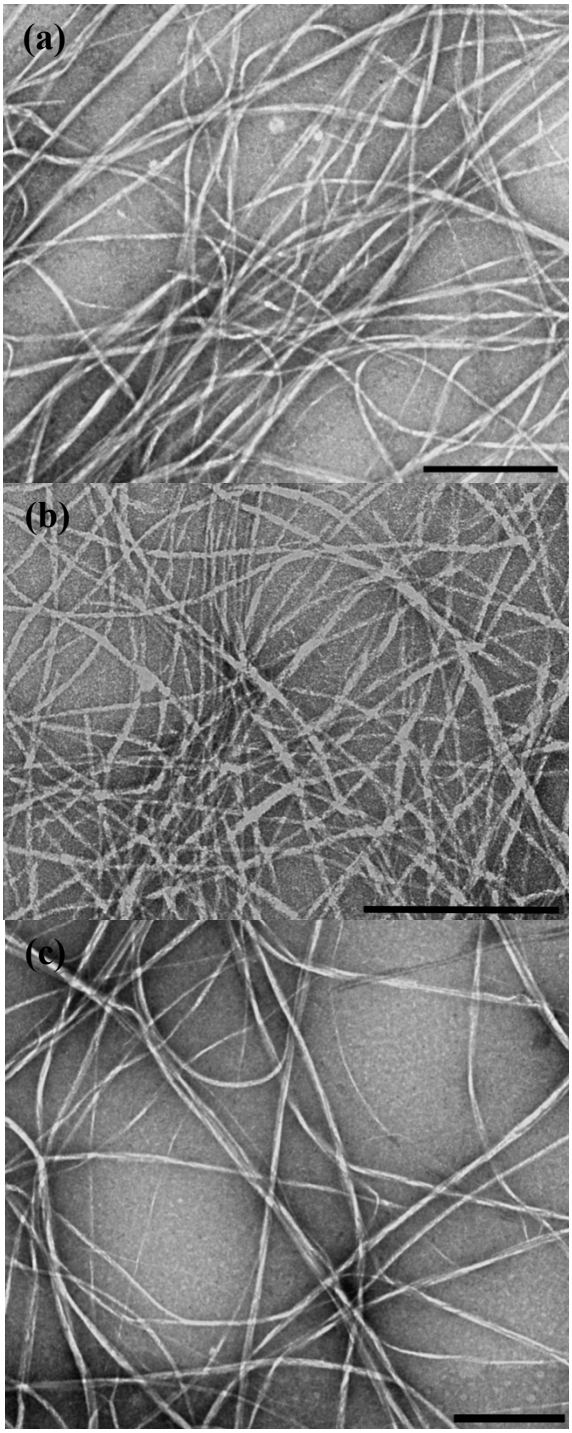

Figure S2: Representative TEM micrographs of nanofilaments observed in the cerium oxide catalysed hydrogelation of FMOC-Tyr-P at concentrations of (a) 25 mM, (b) 12.5 mM, (c) 8.3 mM, scale bar = 500 nm. The filaments are visualized by the presence of a thin film of cerium oxide nanoparticles on the TEM grid; no specific binding of the inorganic nanoparticles to the nanofilaments was observed.

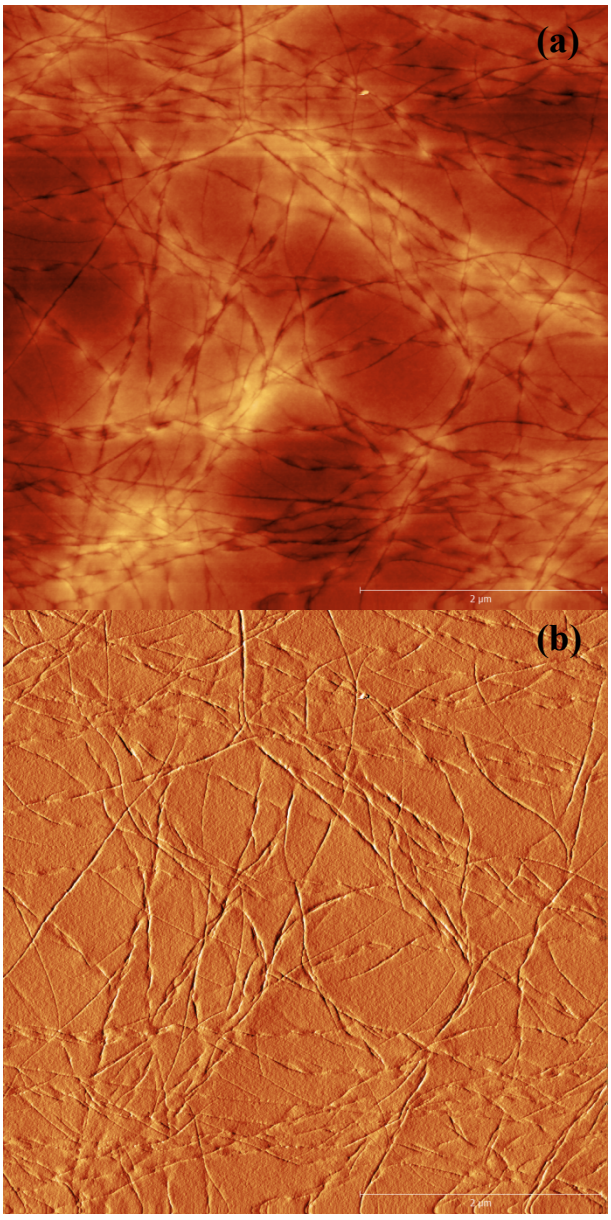

Figure S3: Tapping mode AFM image (a) and corresponding amplitude image (b) of FMOC-Tyr hydrogel (50 mM) showing nanofilaments with twisted ribbon-like morphology.

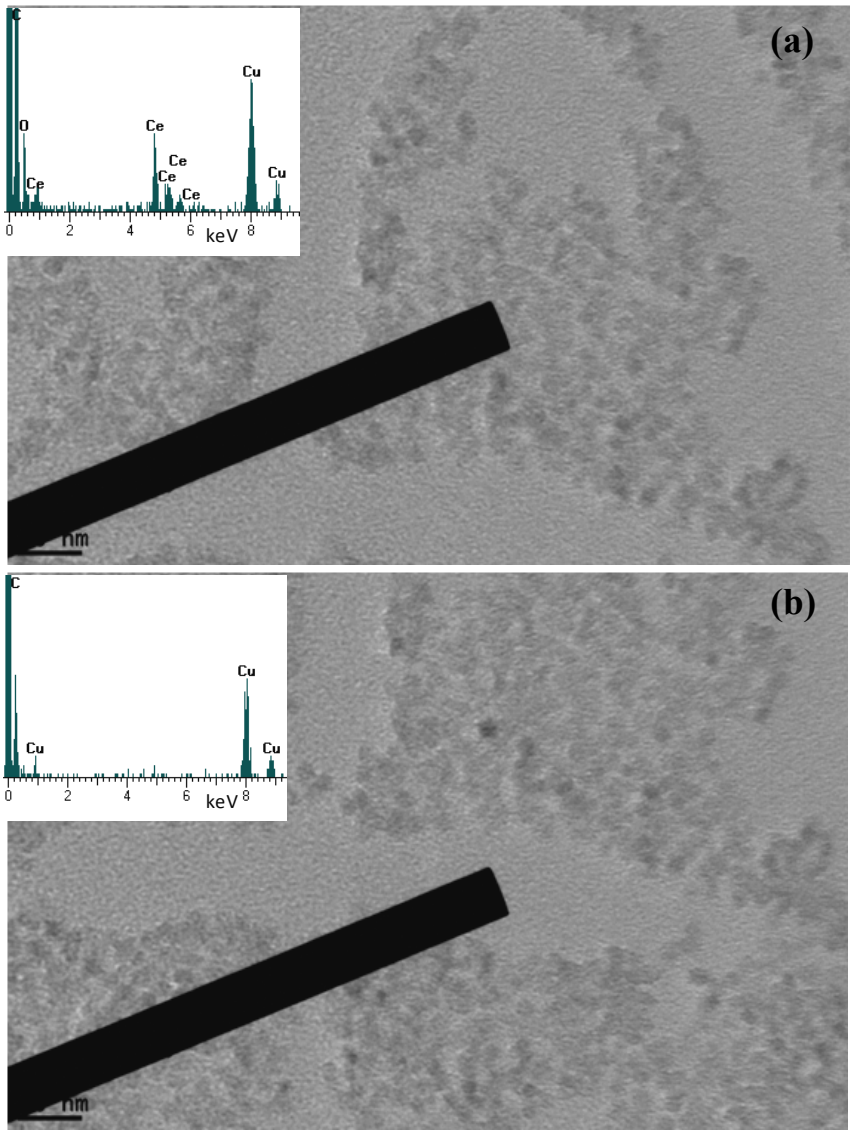

Figure S4: High resolution transmission electron microscopy images of nanofilaments showing deposition of cerium oxide nanoparticles along the edges of the nanofilament (a) and absence of cerium oxide nanoparticles on the surface of most of the nanofilaments (b). Pointer showing areas selected for the energy dispersive x-ray analysis insets showing corresponding data, scale bars = 5 nm.

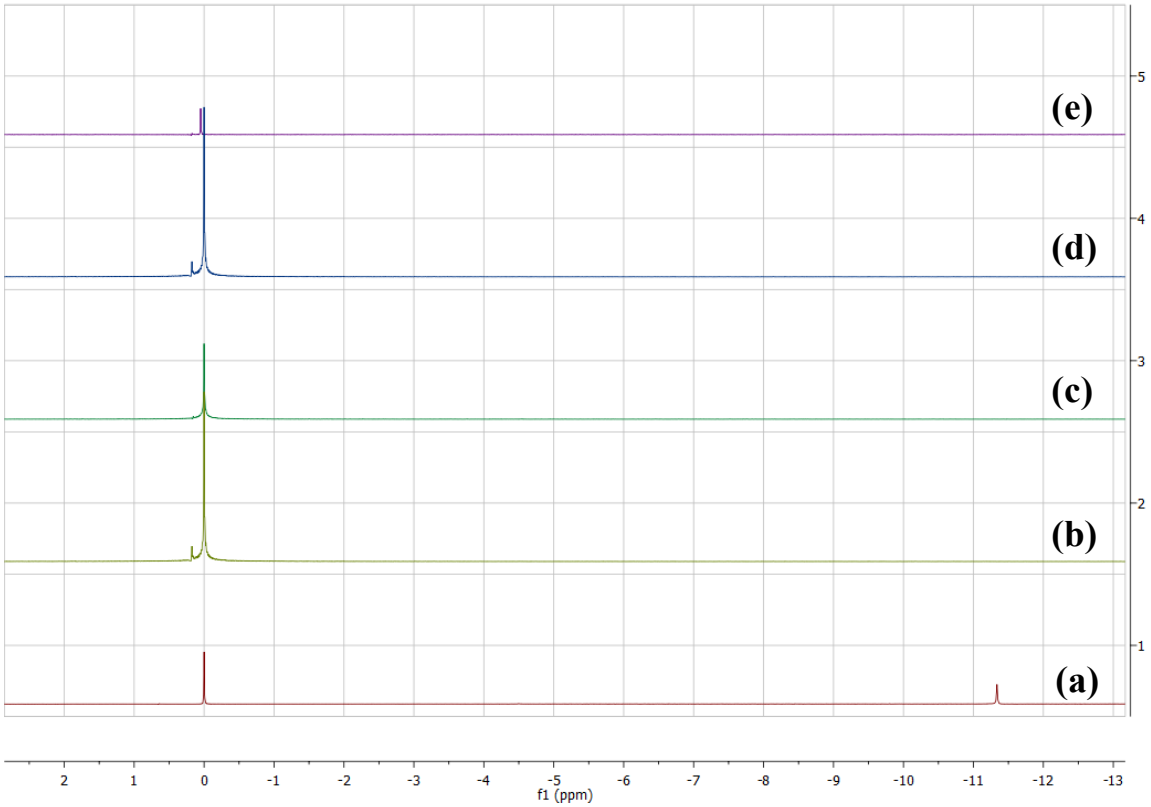

Figure S5: ^{31}P NMR spectra of (a) aqueous FMOC-Tyr-P showing peaks at -11.34 ppm and 0.0 ppm for phosphate ester group and phosphoric acid (internal standard), respectively, and (b)-(e) hydrogel samples produced by cerium oxide nanoparticle-catalysed dephosphorylation of FMOC-Tyr-P at concentrations of 50, 25, 12.5 and 8.3 mM, respectively, showing resonance at 0.17 ppm corresponding to the cleaved phosphate group.

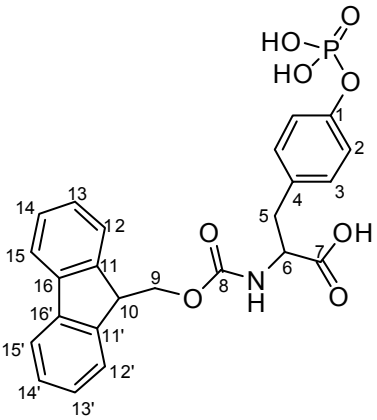

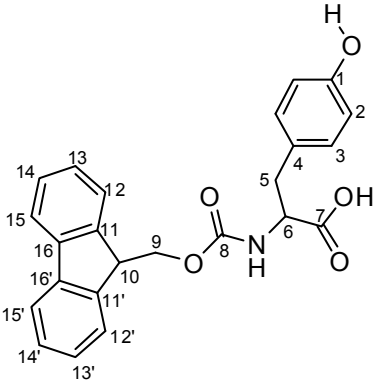

^{13}C NMR (125 MHz, D_2O) of FMOC-Tyr-P: δ_C ppm 37.2 (C5), 47.1 (C10), 59.6 (C9), 61.2 (C6), 120.1 (C2), 120.2 (C15), 120.3 (C15'), 124.9 (C12), 125.1 (C12'), 127.5 (C13), 127.5 (C13'), 128.0 (C14 & C14'), 129.9 (C3), 131.7 (C4), 140.8 (C16), 140.9 (C16'), 142.4 (C1), 143.7 (C11), 143.9 (C11'), 157.4 (C8), 178.5 (C7)

^{13}C NMR (125 MHz, D_2O) of hydrogels: δ_C ppm 37.2 (C5), 47.0 (C10), 59.6 (C9), 61.3 (C6), 120.1 (C2), 120.2 (C15), 120.3 (C15'), 124.9 (C12), 125.1 (C12'), 127.5 (C13), 127.5 (C13'), 128.0 (C14 & C14'), 129.9 (C3), 131.7 (C4), 140.8 (C16), 140.9 (C16'), 143.7 (C11), 143.9 (C11'), 152.1 (C1), 157.4 (C8), 178.6 (C7)

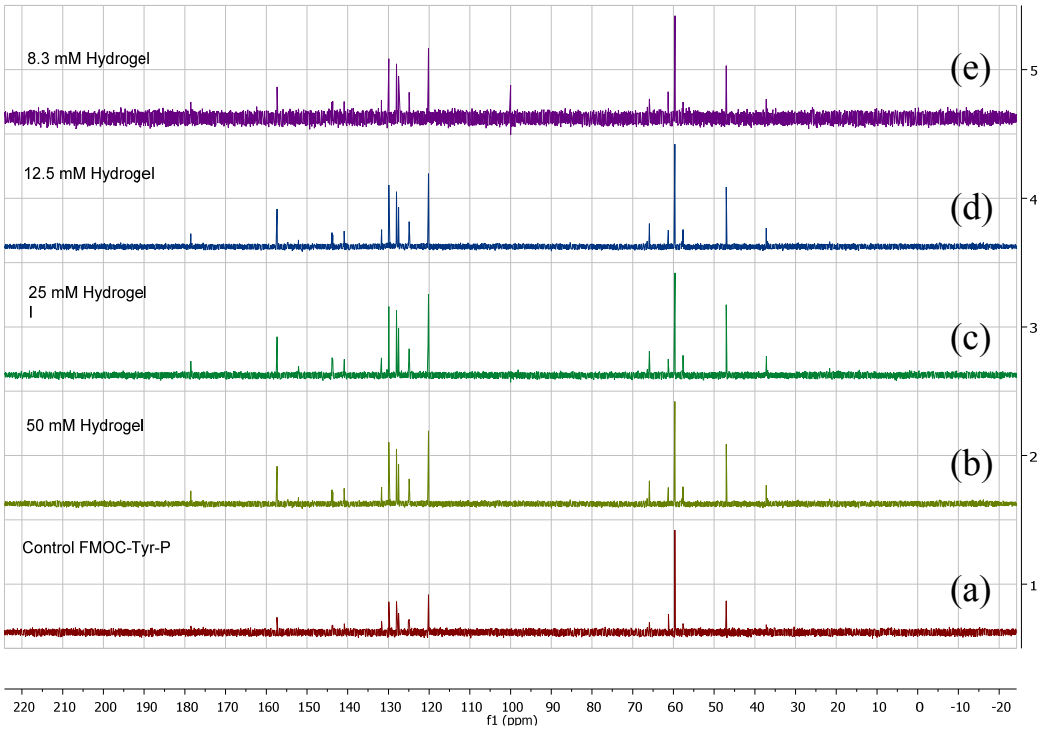

Figure S6: ^{13}C NMR of (a) aqueous FMOC-Tyr-P, and (b)-(e) hydrogel samples produced by cerium nanoparticle-catalysed dephosphorylation of FMOC-Tyr-P at concentrations of 50, 25, 12.5 and 8.3 mM respectively.

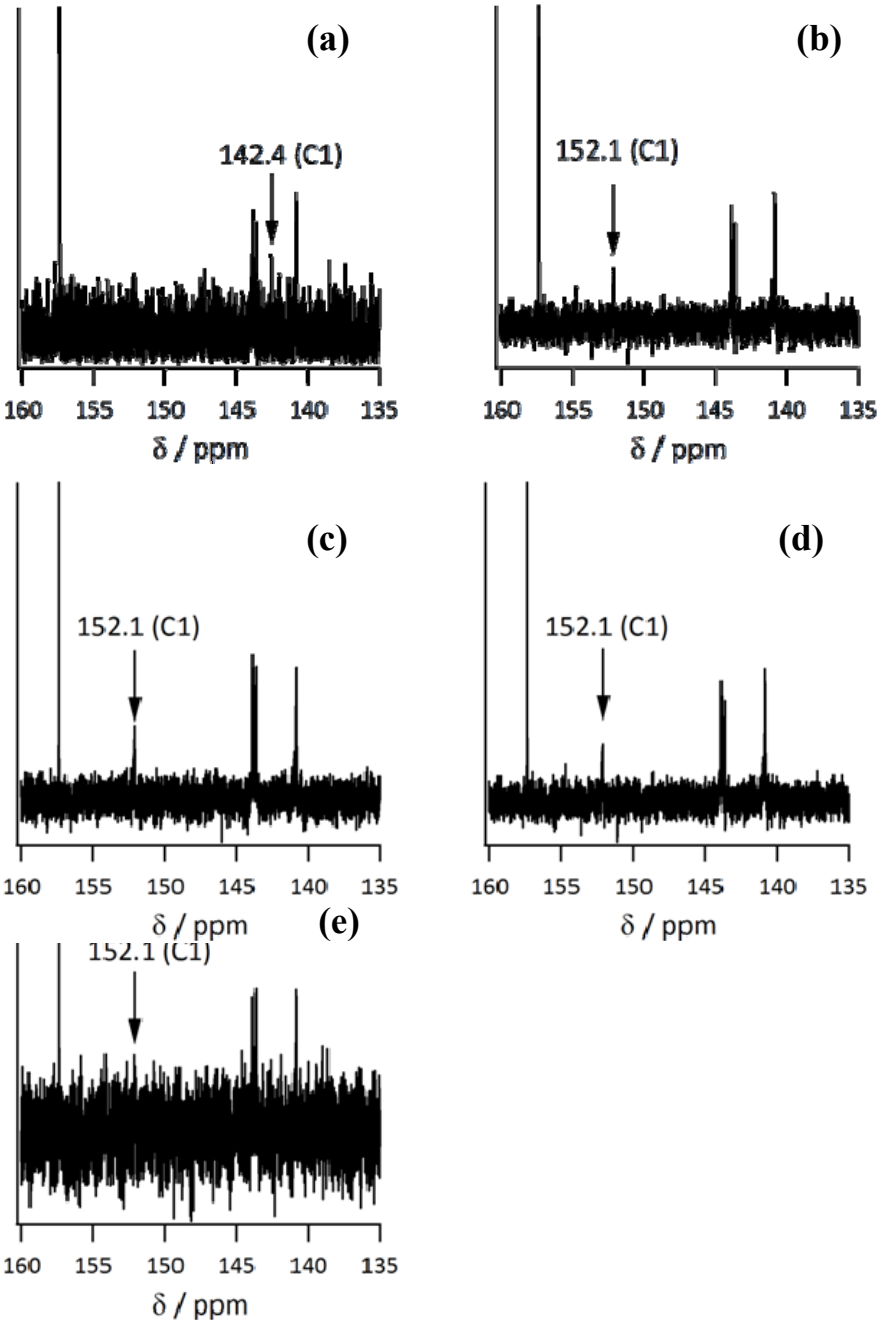

Figure S7: ^{13}C NMR showing (a) resonance at 142.4 ppm associated with C-O-P(O)(OH)$_2$ of FMOC-Tyr-P which on phosphate bond hydrolysis disappeared and a new peak at 152.1 ppm corresponding to C-OH was observed in hydrogel samples at concentrations 8.3, 12.5, 25, 50 mM, (b) to (e) respectively.

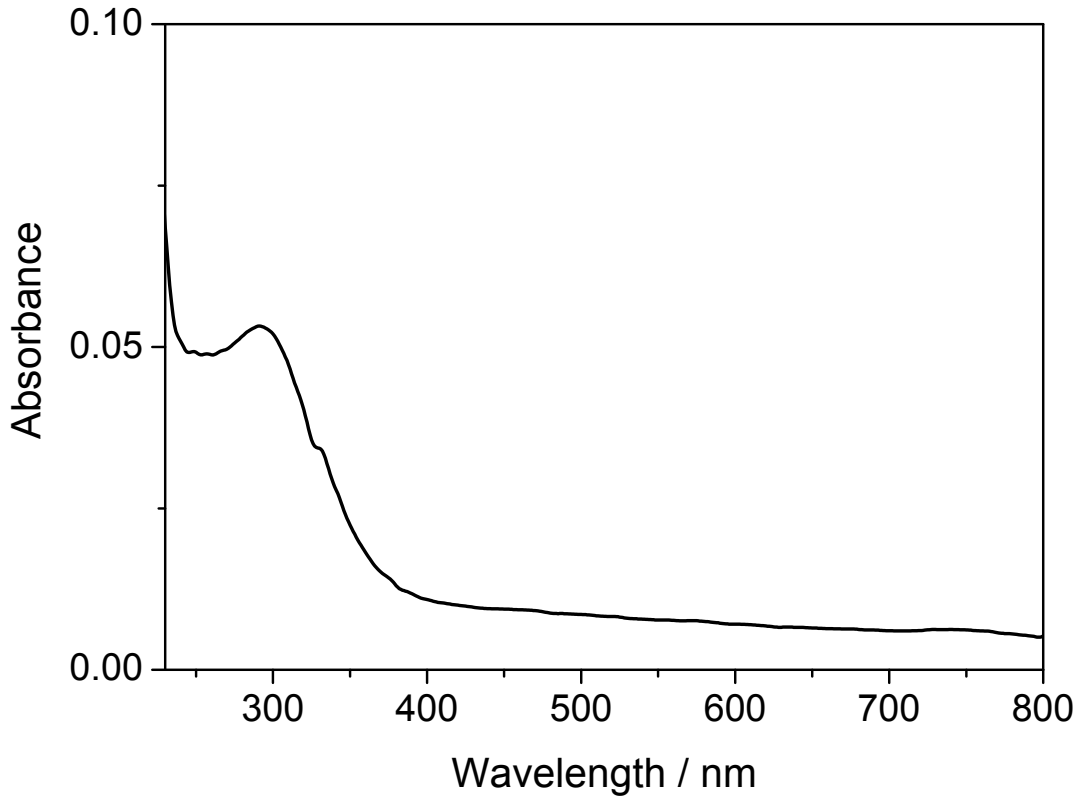

Figure S8: Uv-vis spectrum of aqueous dispersion of CeO_2 nanoparticles.

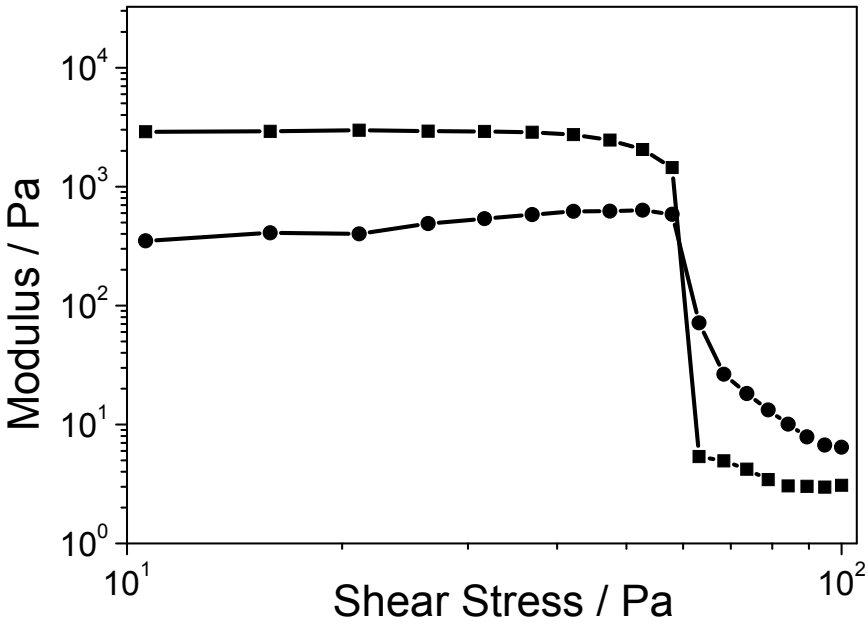

Figure S9: Oscillatory amplitude sweeps at a constant frequency of 1 Hz for hydrogel prepared at 25 mM FMOC-Tyr-P showing linear viscoelastic region for the storage (G', ■) and loss (G", ●) moduli, and structural deformation above a shear stress of 63 Pa.

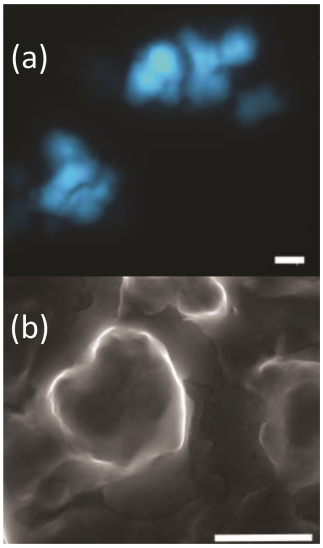

Figure S10: (a) Fluorescence microscopy image showing strong binding of Hoeschst 3325 to the spherulitic domains (b) ESEM image of spherulitic domains; Scale bars = 100 μm.